national accelerator laboratory

NAL-Conf-73/68-EXP
2600.200

(Presented at the APS Meeting, Division of Particles and Fields, Berkeley, Calif., August 13-17, 1973)

DIFFRACTION DISSOCIATION IN pp INTERACTIONS AT NAL

J. Whitmore

September 1973

DIFFRACTION DISSOCIATION IN pp INTERACTIONS AT NAL

J. Whitmore
National Accelerator Laboratory, Batavia, Illinois 60510

ABSTRACT

This report presents a brief summary of the study of diffractive fragmentation in pp collisions as observed in the NAL bubble-chamber experiments. Missing mass, effective mass, and secondary particle rapidity distributions permit a) the study of the multiplicity and t dependences of the diffractive process at high energy, b) the measurement of the cross section for the reaction $pp \to pp\pi^+\pi^-$, and c) an estimate of an upper limit for the double Pomeron exchange contribution to the $p\bar{p}\pi^+\pi^-$ final state at 205 GeV/c.

Diffraction dissociation in pp interactions has been studied in four experiments using the NAL 30-in. bubble chamber. One of the methods available for studying proton diffraction is the effective mass technique which has been profitably employed by the ANL-NAL group[1,2] at 205 GeV/c in analyzing the 4-prong events, in particular, the reaction $pp \to pp\pi^+\pi^-$. The second method which has been used by all three groups, Michigan-Rochester[3] (102 and 405 GeV/c), ANL-NAL[4] (205 GeV/c), and NAL-UCLA[5] (303 GeV/c), is to study the missing-mass reaction:

$$pp \to \text{slow proton} + \text{anything}, \qquad (1)$$

by measuring recoil protons with laboratory momentum below 1.4 GeV/c, a cut imposed by the requirement that the proton be identified visually by bubble density. Such a selection results in a bias against high missing mass (or x) as shown for the 205 GeV/c data[4] in Fig. 1. This scatter plot of x, the Feynman variable, versus P_T, the transverse momentum of the recoil proton, shows a strong elastic band near x = -1 and the circular boundary caused by the 1.4 GeV/c momentum cut. Following removal of the elastic 2-prong events, the missing mass squared (M^2) distributions are shown in Fig. 2 for various beam momenta.[3-7]

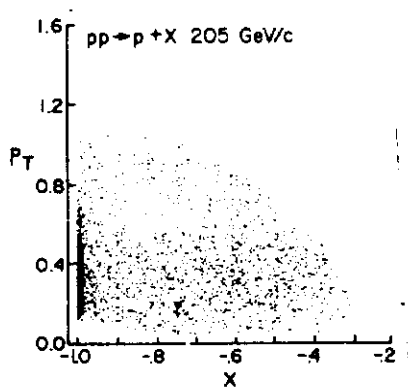

Fig. 1. Scatter plot of x vs P_T for the reaction pp → slow proton + anything at 205 GeV/c.

The dominant features of this figure are

a) the large peak at low M^2,

b) the relatively flat distribution at high M^2,

c) the fall of the peak height as the beam momentum rises from 19 to 102 GeV/c, and the constant height of the peak for the data between 102 and 405 GeV/c, and

d) the greater width of the low mass peak at the NAL energies. It should be noted that since the resolution in M^2 may be approximated by $\pm 0.7\ \text{GeV}^2 \times (P_{lab}/100\ \text{GeV/c})$, this feature implies the observation of proton diffraction into states with masses up to 4 GeV.

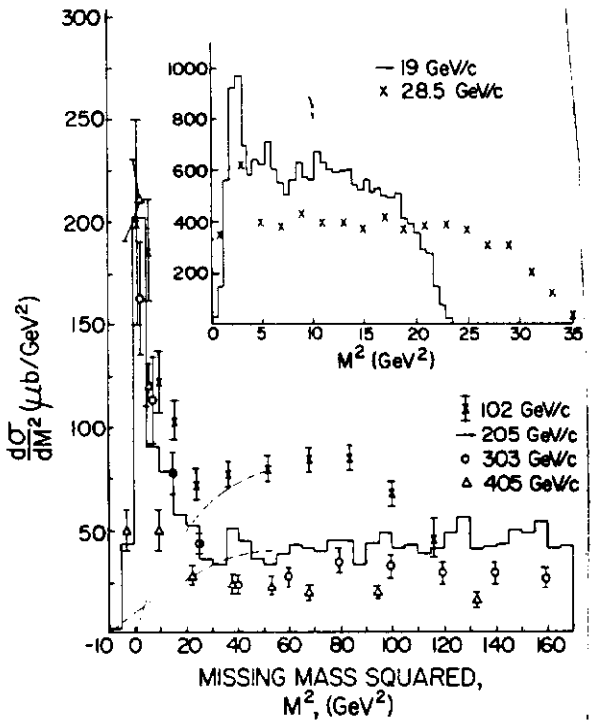

Fig. 2. Missing mass squared distributions for inelastic events in the reaction pp → slow p + X.

The data in Fig. 2 seem to be consistent with a "background" which falls (~1/s, see Fig. 4 below) and a low mass enhancement with a cross section for $M^2 \lesssim 20\ \text{GeV}^2$ which is energy independent. In order to obtain cross sections for this this low mass peak, the ANL-NAL group has estimated the number of events above the hand-drawn background in Fig. 2. Using similar estimates for the shape of the background at each of the other energies, the resulting cross sections for single diffraction, σ_s, are

P_{lab}(GeV/c)	σ_s(mb)
19	2.15±0.30
28.5	1.70±0.30
102	2.50±0.35
205	2.60±0.30
303	2.15±0.25
405	2.05±0.25.

The cross section for low mass single diffraction thus appears to be relatively constant with a value ~2.2±0.5 mb.

To study the multiplicity dependence of this low mass peak, the missing mass squared distributions are shown in Fig. 3 for the individual topologies at 205 GeV/c (similar distributions are observed at the other energies) and indicate that (44±6)% of σ_s is due to the 2-prongs, (46±5)% to the 4-prongs, and (10±3)% to the 6-prongs.[4] A noticeable feature of Fig. 3 is that the position of the peak increases in M^2 as the charged multiplicity increases. There are no

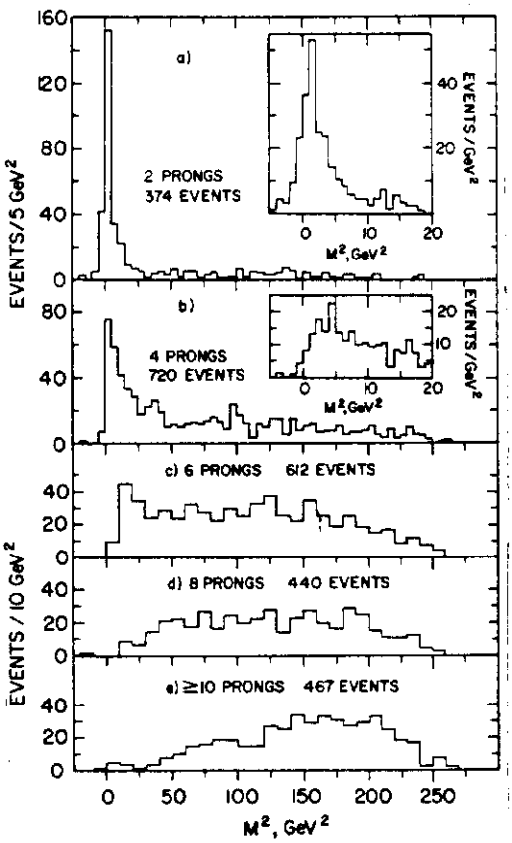

Fig. 3. Missing mass squared distributions at 205 GeV/c for various topologies.

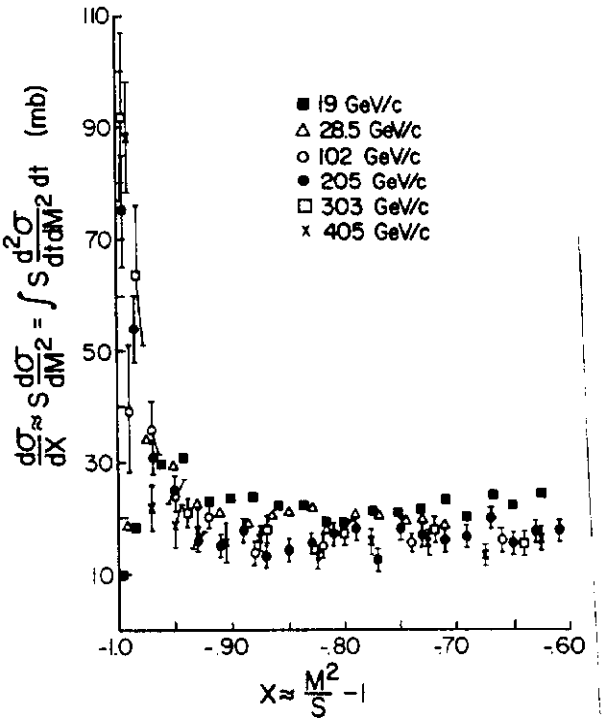

Fig. 4. Inclusive proton differential cross sections as a function of x.

significant peaks for events with 8 or more prongs. Thus the cross sections quoted above represent lower limits on the diffractive fragmentation of the beam proton since it is hard to estimate contributions from diffractive processes leading to high M^2 states or yielding distributions that do not peak at low mass.

These slow proton data[3-7] may also be presented in terms of their x dependence as shown in Fig. 4 which indicates that for $x \lesssim -0.95$ the cross section is rising with energy. For $x \gtrsim -0.95$ there is perhaps a trend for a falling cross section as s increases up to NAL energies, although the cross section shows little energy dependence within the NAL region.

The t dependence of process (1) is further indication that the low mass peak is diffractively produced. Figure 5 shows the invariant cross section for several ranges of M^2 at 205 GeV/c.[4] Except for the regions affected by the kinematics at high M^2, all of the distributions can be well represented by an exponential t dependence.

The effective mass analysis has provided further information about the low mass peak. Figure 6(a) shows the missing mass

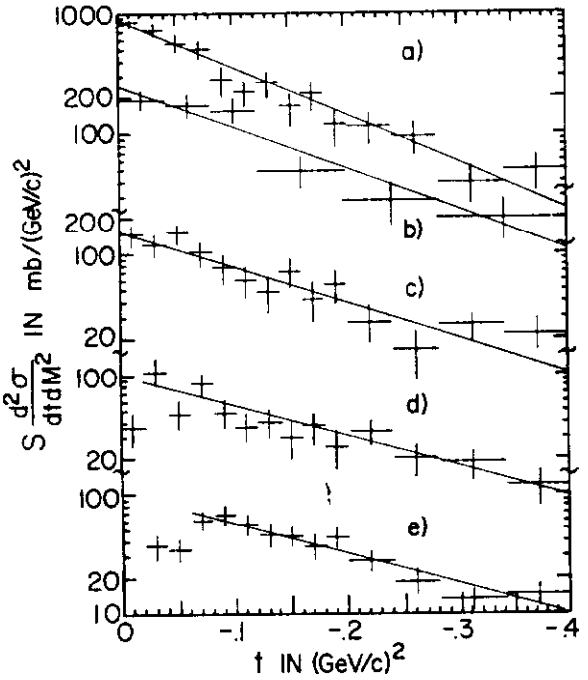

Fig. 5. Invariant cross section vs four-momentum transfer squared, t, for various ranges of missing mass squared at 205 GeV/c. The lines are the results of fits to the form A exp(bt). (a) $M^2 < 5$ GeV^2 $b = 9.1 \pm 0.7$ (GeV/c)$^{-2}$. (b) $5 \leq M^2 < 10$ GeV^2, $b = 8.0 \pm 1.1$ (GeV/c)$^{-2}$. (c) $10 \leq M^2 < 25$ GeV^2, $b = 6.1 \pm 0.7$ (GeV/c)$^{-2}$. (d) $25 \leq M^2 < 50$ GeV^2, $b = 5.8 \pm 0.7$ (GeV/c)$^{-2}$. (e) $50 \leq M^2 < 100$ GeV^2, $b = 5.8 \pm 0.6$ (GeV/c)$^{-2}$.

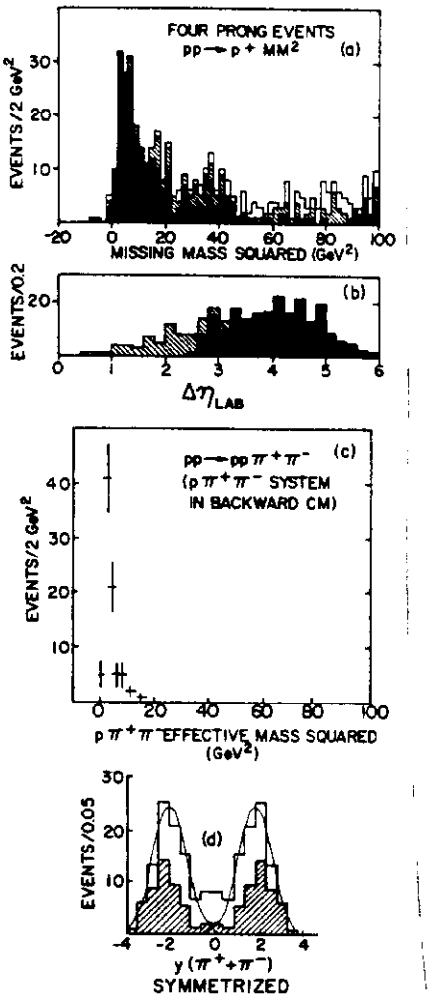

Fig. 6(a). Missing mass squared distribution for 4-prongs at 205 GeV/c. (b) Distribution of the rapidity gap between the leading proton and its nearest neighbor for $M^2 \leq 50$ GeV^2. (c) $p\pi^+\pi^-$ effective mass squared distribution for the reaction $pp \rightarrow pp\pi^+\pi^-$ at 205 GeV/c. (d) Center-of-mass rapidity distribution (after symmetrization) for the $\pi^+\pi^-$ system.

squared distribution for reaction (1) for the 4-prong sample at 205 GeV/c.[1] The shaded (cross-hatched) area shows the sub-sample of events in which just 3 (2) charged particles are in the forward c.m. hemisphere and indicates that most of the enhancement at low M^2 is associated with one backward c.m. proton and 3 forward c.m. charged particles. Since one might expect that diffractive events would show up in the ordered rapidity distribution with a large gap, associated with Pomeron exchange, Fig. 6(b) shows the distribution of the rapidity gap between the leading (i.e., slow)

proton and its nearest neighbor, where the pseudorapidity $\eta = \ln \tan(\theta_{lab}/2)$ has been used. The events with 3 forward c.m. particles have an average gap length of ~5 units, while those with 2 forward tracks usually have a smaller gap. Although having $M^2 \leq 50$ GeV^2, these latter events cannot be considered diffractive since this gap is the largest gap in the event for only 32 of the 58 events in the plot.

To further study the various contributions to the low M^2 peak in the 4-prong events, an effort has been made to determine those events consistent with the process

$$pp \rightarrow pp\pi^+\pi^-. \qquad (2)$$

By using those events in which there are 3 slow backward c.m. tracks and one forward c.m. charged track, a relatively clean sample, with an estimated 30% or less contamination, of events fitting (2) has been obtained. Derrick et al.[1,2] find a cross section for reaction (2) at 205 GeV/c of $0.85\ ^{+0.09}_{-0.29}$ mb. The $p\pi^+\pi^-$ effective mass for these fitted events is shown in Fig. 6(c) and should be compared to Fig. 6(a). The peak due to $pp\pi^+\pi^-$ is confined to the low mass part of the total 4-prong peak and, furthermore, indicates that only ~35% of the 4-prong peak is due to reaction (2). This implies that the dominant contribution to the 4-prong peak is due to events with 5 or more particles in the final state. Further evidence of this is shown in Fig. 7 for those events in which three slow π's are identified in the backward c.m.[1] The rapidity, η_F, of the remaining charged track is plotted versus the rapidity gap, Δ, between this track and its nearest charged neighbor. The cluster of ~30 events with $\Delta \sim 5$ and $\eta_F \sim 6.5$ is indicative of diffractive fragmentation of the target proton into high multiplicity states, such as $n\pi^+\pi^+\pi^-(m\pi^0)$ with $m \geq 0$.

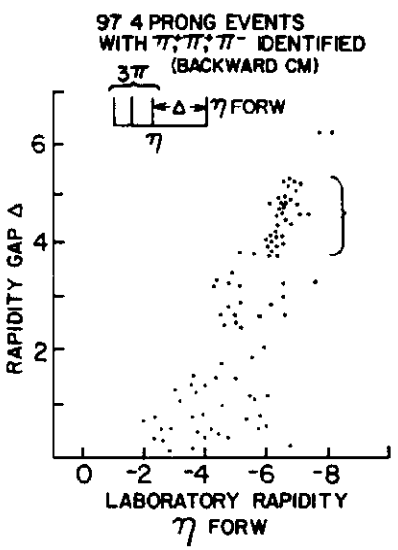

Fig. 7. Scatter plot of the leading particle rapidity, η_F, vs the rapidity gap, Δ, between it and its closest neighbor for those 4-prongs with π^+, π^+, π^- identified by ionization.

Further rapidity analysis[2] has yielded an estimate for the double Pomeron (DP) exchange contribution to reaction (2). The dominant features of this reaction are a low $p\pi^+\pi^-$ effective mass enhancement, the strong production of $\Delta^{++}(1236)$ associated with the low mass $p\pi^+\pi^-$ peak,[9] and the peripherality of the $p\pi^+\pi^-$ system. For $p\pi^+\pi^-$ masses less than 3 GeV and $0 < |t| < 0.35$ (GeV/c)^2, the data are well

represented by an exponential t dependence with slope b = 9.1±1.0 $(GeV/c)^{-2}$.

To obtain the DP contribution, Derrick et al.[2] note that the effective mass of the $\pi^+\pi^-$ system tends to lie below the ρ mass, the helicity angular distribution of the 2π system is isotropic, and the rapidity of the 2π system has a double-peaked structure [Fig. 6(d)]. These features suggest that the 2π system results from the diffractive fragmentation of either the beam or target proton. Since any DP contribution would be expected to occur in the central 2 units of Fig. 6(d), an estimate of the events[9] above a fit with 2 gaussians [shown as the curve in Fig. 6(d)] yields an upper limit of 45 μb for the the DP contribution. A similar result at 24 GeV/c[10] gave a 30 μb upper limit for 2π effective masses less than 0.6 GeV. For a similar dipion mass cut [shown as the cross-hatched area in Fig. 6(d)], an upper limit of 35 μb (7 events) is obtained at 205 GeV/c.[2]

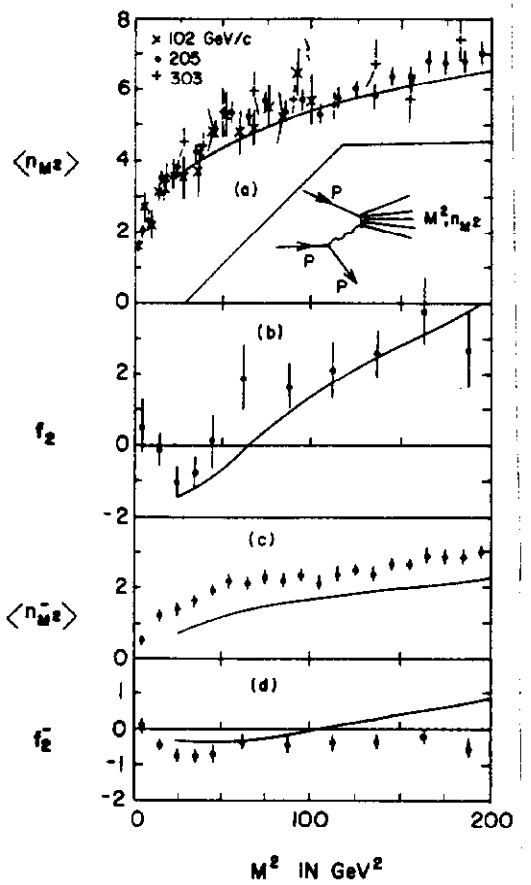

Fig. 8. Multiplicity moments of the charged system X in the reaction pp → slow proton + X plotted versus M^2. (a) $\langle n_{M^2} \rangle$, (b) f_2, (c) $\langle n^-_{M^2} \rangle$ and (d) f_2^-. The curve curves show the dependences on s of these quantities for real pp collisions.

Finally, Fig. 8(a) shows[4] the average multiplicity $\langle n_{M^2} \rangle$ for the charged particles recoiling against the slow proton in reaction (1) at 102, 205, and 303 GeV/c.[3-5] No strong dependence on beam energy is observed. The curve in Fig. 8(a) is obtained from a fit[11] to the s dependence of the charged particle multiplicity (in pp → n charged particles) with the result $\langle n \rangle = -4.8 + 2\ell n s + 10/\sqrt{s}$. For Fig. 8(a) the substitution $s = M^2$ has been made. Although the data lie systematically above the curve, they do show a remarkably similar energy dependence. Various other moments are also shown in Fig. 8.

It is tempting to suggest[4] that if reaction (1) proceeds via single particle exchange [insert in Fig. 8(a)], then studying $\langle n_{M^2} \rangle$ as a function of M^2 is equivalent to studying exchanged particle-proton interactions as a function of s. It should be noted, however, that only for $M^2 \leq 20$ GeV^2

can Fig. 8(a) be considered as describing Pomeron-proton collisions.

REFERENCES

1. M. Derrick et al., Diffraction Dissociation in Proton-Proton Interactions at 205 GeV/c, ANL/HEP 7332 (1973).
2. M. Derrick et al., An Estimate of the Double Pomeron Exchange Contribution to the Reaction $pp \rightarrow pp\pi^+\pi^-$ at 205 GeV/c, ANL/HEP 7339 (1973).
3. Michigan-Rochester collaboration, private communication from A. Seidl and J. VanderVelde.
4. S. J. Barish et al., Characteristics of the Reaction $pp \rightarrow p + X$ at 205 GeV/c, ANL/HEP 7338 (1973).
5. NAL-UCLA collaboration, private communication from F. T. Dao.
6. Scandinavian collaboration, private communication from H. Bøggild.
7. BNL-Vanderbilt collaboration, private communication from J. Hanlon.
8. The resolution in the $p\pi^+\pi^-$ effective mass squared is much smaller than 1 GeV^2, see Ref. 1.
9. Substantial Δ^{++} production in the 4-prong events has also been observed at 303 GeV/c, F. T. Dao et al., Phys. Rev. Letters 30, 34 (1973).
10. V. Idschok et al., DESY preprint, submitted to Nucl. Phys. B (1973).
11. D. M. Tow, Phys. Rev. D7, 3535 (1973).